JPG Journal of Petroleum Geology www.jpg.co.uk

Journal of Petroleum Geology, Vol. 40(3), July 2017, pp 277 - 297

BURIAL HISTORY AND THERMAL MATURITY EVOLUTION OF THE TERMIT BASIN, NIGER

M. Harouna[1]*, J. D. Pigott[2] and R. P. Philp[2]

Reconstruction of the burial history and thermal evolution of the Cretaceous – Tertiary Termit Basin, a sub-basin within the larger Eastern Niger Basin of Niger, indicates spatially and temporally variable conditions for organic matter maturation during the basin's multi-phased evolution. Three episodes of tectonic subsidence which correspond to the observed fault mechanical stratigraphy within the Termit Basin are identified: Late Cretaceous, Maastrichtian to early Paleocene, and Oligocene. These episodes fall within the regional tectonic phases of the West African Rift System delineated by previous studies. The basin exhibits substantial heterogeneity in the magnitude of the tectonic episodes and in consequent thermal maturities. For this paper, 1D burial and thermal histories of eight widely dispersed wells in the Agadem permit area in the SW of the Termit Graben were modelled to investigate the maturation of organic matter in source rocks ranging from Santonian to Oligocene in age. The kinetic modelled maturities match with maturities based on Rock-Eval T_{max} values for four wells if present-day heat flows are elevated. Future exploration strategies in the Termit Basin should take into consideration these heterogeneities in thermal histories and tectonic pulses, which may lead to the development of hydrocarbon accumulations with different oil-gas compositions in different reservoir compartments.

INTRODUCTION

The underexplored Termit Basin, a Cretaceous – Tertiary multi-rift graben, is located in the larger Eastern Niger Basin (Fig. 1). Preliminary exploration included studies by Esso Exploration and Production Niger Inc. and partners who up to 2006 had acquired more than 15,000 line km of seismic data together with some 30 thousand km of aeromagnetic lines, and had drilled more than 20 exploration wells. More recently, exploration by China National Petroleum Corporation (CNPC) has continued in the Agadem permit area, which covers about 27,000 km^2 in the SE of the graben (Fig. 1). The presence of good to excellent source rocks (Harouna and Philp, 2012) together with high quality reservoirs and seals (Genik, 1992; Liu *et al*., 2017), as well as the history of production which began with a 1974 discovery by Conoco (MBendi Information, 2010) and the recent discoveries of Kanem, Lumia, and Seidigi oilfields (Gaya, 2013) confirm the Termit Basin's hydrocarbon prospectivity. One recent study estimated that the Ténéré graben (to the NW of Termit: Fig. 1) contains approximately 500 million barrels

[1] Université Abdou Moumouni, Faculté des Sciences et Techniques, Département de Géologie, B.P. 10662 Niamey, Niger.
[2] The University of Oklahoma, Conoco-Phillips School of Geology & Geophysics, Norman, Oklahoma, 73019 OK, USA.

* corresponding author, email: mharounam@gmail.com

Key words: Termit Graben, Eastern Niger Basin, Niger, source rocks, maturity, thermal modelling

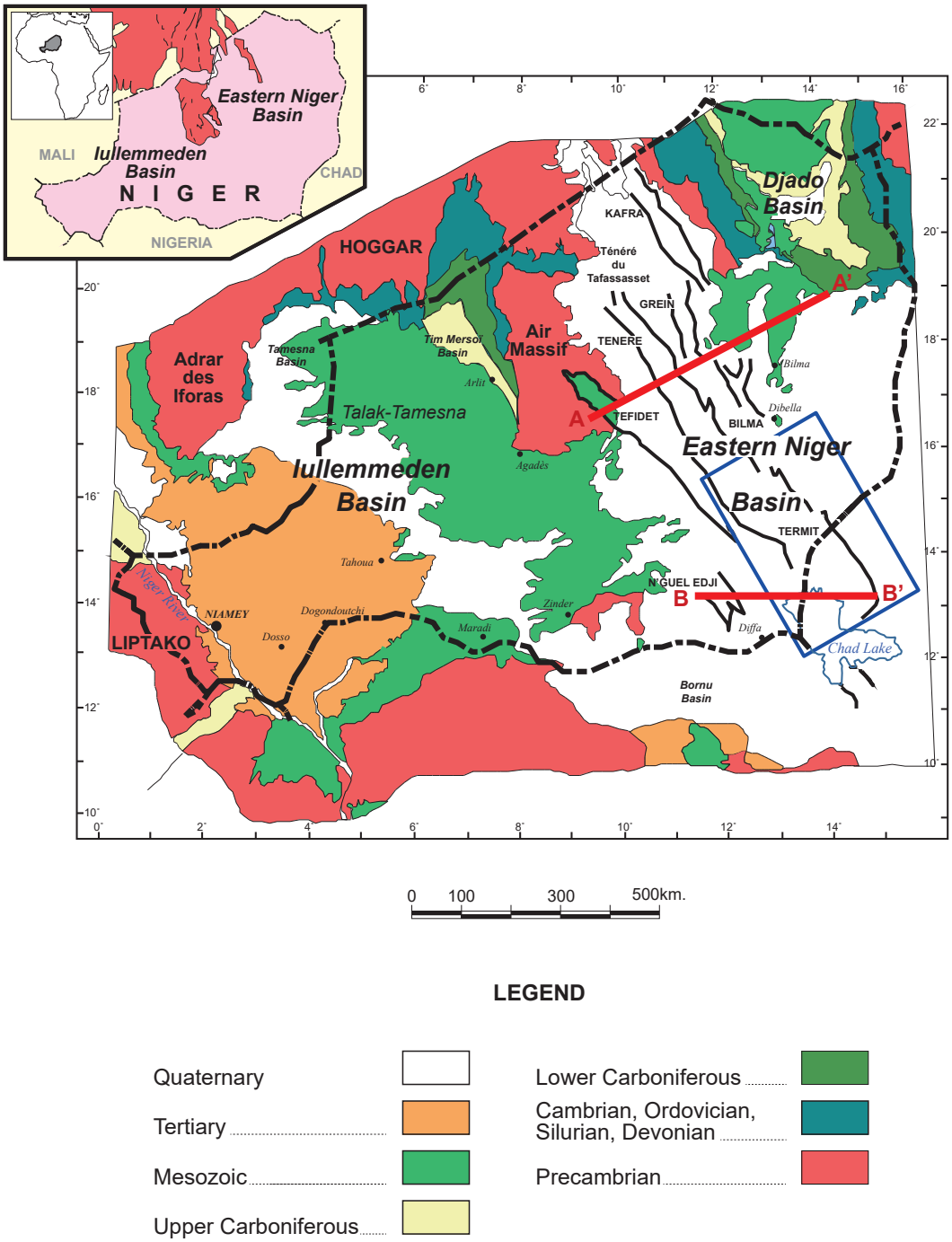

Fig. 1. Geological map of Niger with the location of the Eastern Niger graben system (Harouna and Philp, 2012). The red dashed lines refer to the locations of the cross-sections shown in Figs 3 and 4. The black dashed line shows country borders. The blue box outlines the approximate location of the Termit Basin.

of oil-equivalent in nine oil discoveries and one gas discovery (TG World Petroleum Ltd, 2009).

A preliminary source rock assessment of the Termit Graben based on organic geochemical studies (Rock-Eval, bitumen extract and biomarker analyses) was published by Harouna and Philp (2012), and biomarker and isotopic studies were presented by Wan *et al.* (2014). However, questions remain concerning the evolution of the petroleum system in the graben. For example, organic geochemical studies including Rock-Eval T_{max} values, sterane ratios and homohopanes led Liu *et al.* (2015) to suggest that the Middle Upper Cretaceous source rocks have reached the early oil generation window. But it is not clear when the maturation occurred and or how it is related to the two or more tectonic phases which have been identified (Genik, 1992). Therefore the purpose of the present paper is to further investigate the petroleum system in the Termit Graben in terms of the burial history, thermal history and timing of hydrocarbon generation, and to attempt to relate the system's evolution to phases of crustal rifting. Maturity information obtained from

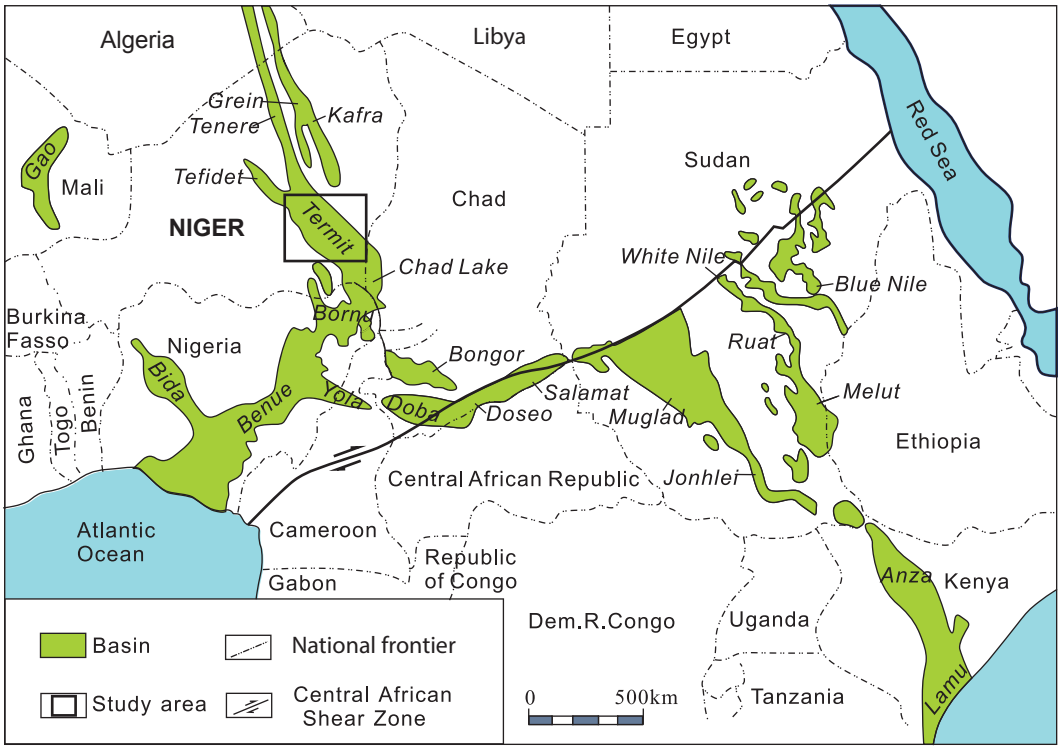

Fig. 2. Map showing the West and Central African Rift System (WCARS) with the location of the Eastern Niger graben system (after Genik, 1993). The box outlines the approximate location of the Termit Basin.

previous organic geochemical studies (including Harouna and Philp, 2012) was used to calibrate the numerical models.

Geological Setting

The Eastern Niger Basin (also known as the Chad Basin) extends some 1000 km north-south and 700 km east-west in the eastern part of the Republic of Niger (Fig. 1) and has more than 14 km of sedimentary fill (Genik, 1992). To the west and NW the basin is bounded by crystalline basement rocks of the Precambrian Gouré and Aïr and Mesozoic Zinder massifs; to the north by the Quaternary Ténéré du Tafassasset massif; and to the east and NE by the Mesozoic Dibella Granite (Genik, 1992). The Eastern Niger Basin is a composite basin made up of several narrow sub-parallel grabens (Figs 1 and 2). To the north of the 17th parallel are the Ténéré, Grein, Kafra and Bilma grabens, while to the south are the Termit Graben with its SW extension, the N'Guel Edji Graben.

The grabens in Eastern Niger are part of the West African rift system which, together with the Central African rift system within Chad, the Central African Republic and Sudan, form the West – Central African rift system (Fig. 2) (Genik, 1992, 1993; McHargue *et al.*, 1992; Schull, 1988; Fairhead, 1986). This rift system extends from Mali to Kenya and developed during the break-up of Gondwana in the Early Cretaceous. In the Niger grabens, Genik (1993) recognized six major tectonic phases: two pre-rift; three synrift (two during the Cretaceous and one in the Paleogene); and a post-rift phase (Genik, 1993).

The Eastern Niger graben system was first identified from an interpretation of negative gravity anomalies (Rechenman, 1967, 1969; Louis, 1970), and was subsequently confirmed by surface mapping and wells which delineated six approximately *en échelon* grabens (Figs 1 and 2). These are:

- the Téfidet Graben, which contains Lower Cretaceous and marine Cenomanian–Turonian siliciclastic sediments (Faure, 1966) and which extends for a length of about 400 km;
- the Ténéré Graben, where well Fachi-1 penetrated the Lower Cretaceous at 3740 m and where the Eocene – Oligocene sediments are absent owing either to erosion (Zanguina *et al.*, 1998) or non-deposition.
- the Grein-Kafra Graben, which extends for >600 km from the Algeria–Niger frontier SE to Dibella, and which contains a 3000–4000 m thick Cretaceous – Tertiary succession (Zanguina *et al.*, 1998);
- the Bilma Graben, which contains an 800 to 1000m thick Cretaceous – Tertiary sedimentary package overlying a presumed Lower Cretaceous or Permo-Triassic substratum.
- the relatively shallow N'Guel Edgi graben, located to the west of the southern tip of the Termit Graben, and which is about 100 km long and 40 km wide;
- and the Termit Graben, the focus of this paper, which is over 400 km long and approximately 200 km wide.

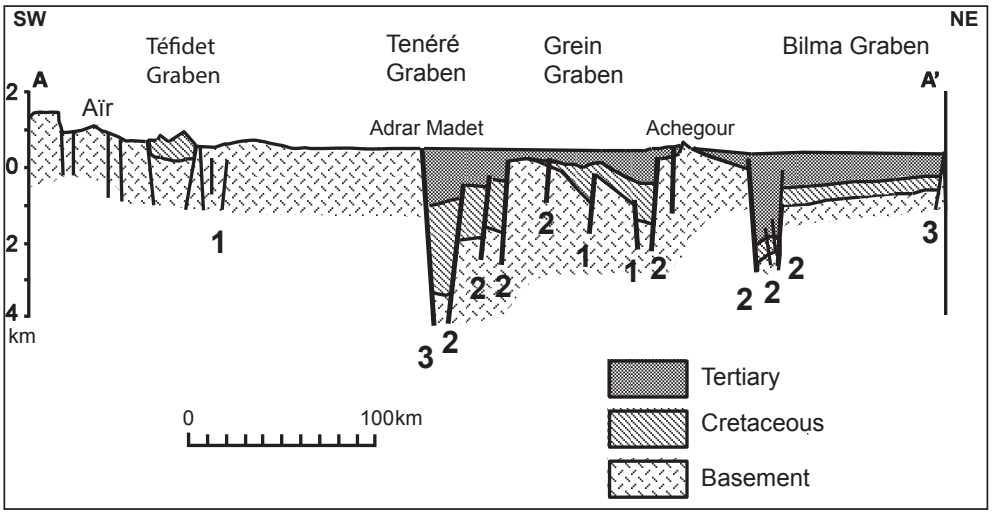

Fig. 3. Cross-section through the Téfidet, Ténéré, Grein and Bilma grabens (after Zanguina *et al.*, 1998). Faults designated by numbers refer to their association with the episodes of crustal extension described in the text. Cross-section profile in Fig. 1.

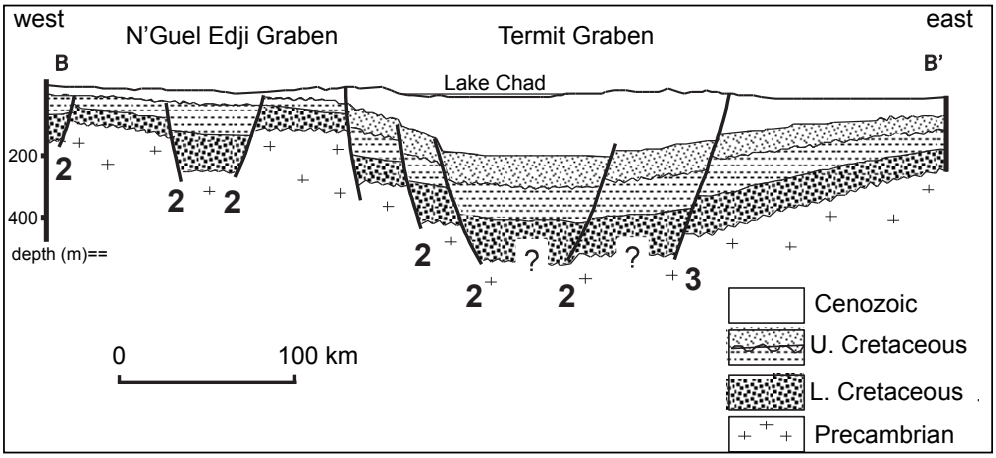

Fig. 4. Cross-section through the Termit and N'Guel Edji grabens (after Bellion, 1987). Faults designated by numbers refer to their association with the episodes of crustal extension described in the text. Cross-section profile in Fig. 1.

Within the Termit Graben, exploration wells have penetrated up to 2000 m of post-Paleocene sediments in well Sokor-3 and over 3800 m of Lower Cretaceous in well Madama-1. The Yogou-1 well reached a depth of approximately 4000 m and is the deepest exploration well drilled in the eastern Niger Basin.

Structural cross sections (Figs 3 and 4, after Zanguina *et al.*, 1998) reveal the elongated asymmetric grabens within the Termit Basin to be bounded by three populations of NW-SE striking normal fault systems of differing ages. These faults indicate three episodes of extension. Episode 1 is syn-Cretaceous (faults pierce Cretaceous strata); Episode 2 is Maastrichtian to Early Paleocene (faults pierce the Cretaceous but not the Tertiary); and Episode 3 is post-Cretaceous (faults pierce the Tertiary). This interpreted fault mechanical stratigraphy is geomechanically plausible as tectonic faults propagate upwards owing to vertically decreasing stratal layer strength elastic moduli (Pigott and Abouelresh, 2016). How the evolution of these three fault pulses affected the Termit Basin and the thermal maturity of the source rocks is at the core of this investigation.

AVAILABLE DATA

Data Sources and Procedure

Eight wells in the Agadem permit area in the SW portion of the Termit Graben are analyzed for burial-thermal histories using BasinMod software (Platte River Associates, Inc.). From generally south to north, the wells are Yogou-1, Sokor-1, Faringa-1, Goumeri-1, Boujamah-1, Karam-1, Sountellane-1 and Soudana-1 (locations in Fig. 5). With respect to source rocks, six Oligocene samples were analysed together with 21 Eocene samples, 12 Paleocene samples, three Maastrichtian – Campanian samples, and eight Santonian samples.

Input data used for the modelling were collected from well-completion reports supplied by Esso

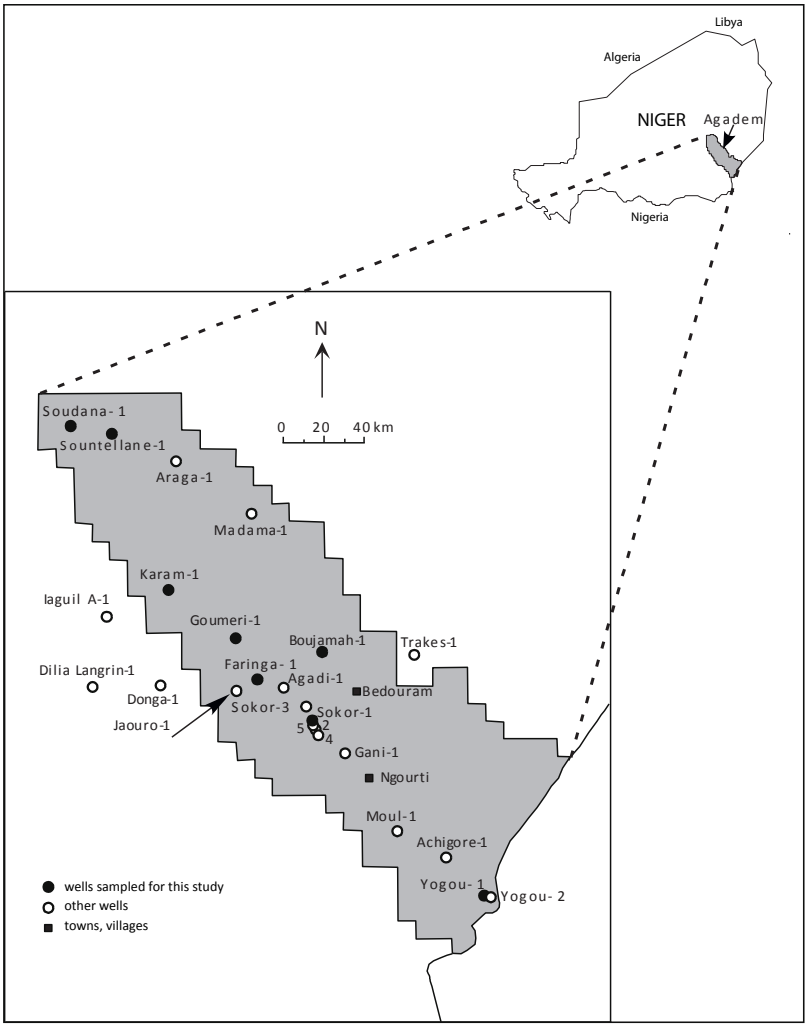

Fig. 5. Map of the Agadem permit in the Termit Basin showing the locations of exploration wells (Harouna and Philp, 2012); black circles show the eight wells considered in this study.

Exploration & Production Niger, Inc. Input data used for burial and thermal history modelling included stratigraphic data, present-day geothermal parameters, and thermal maturities (Table 1). Stratigraphic data included the present-day thickness of stratigraphic intervals, lithologies, tops, and ages which were derived from well-completion reports (Tables 2 – 9). As the existing formation names were lithostratigraphically determined and consequently vary in composition throughout the Termit Basin and as the formation ages of the strata better facilitate time correlation, ages rather than formation names will be used in the modelling.

The stratigraphic modelling takes into account three principal end-member lithologies (sandstones, shales and limestones) with the average lithological contents estimated as percentages for formations with mixed lithologies with corresponding mixed parameters (compaction constants, thermal conductivities, etc.). Rather than use the raw borehole temperatures which would seriously underestimate thermal conditions, a temperature correction was required. But as borehole temperatures with associated circulation times and times after the cessation of circulation were unavailable, Horner plot corrections (Dowdle and Cobb, 1965) to the observed temperatures could not be made. Instead, raw bottom-hole temperatures were corrected via the empirical method of Achraf *et al.* (2015), which compared Drill Stem Tests to raw borehole temperatures in the Jaffara Basin which is located in southern Libya and Algeria. Heat flows in the Termit Basin were calculated from the borehole-corrected temperatures and surface temperatures using a harmonic average of mixed thermal conductivities which corresponded to the mixed borehole lithologies via BasinMod.

Palaeoheat flows were determined by backtracking current heatflows and then forward modelling at crustal stretching factor increments which were calculated from the tectonic subsidence. The tectonic subsidence was determined from burial history curves after removing the effects of isostasy and sea level changes (see Metawalli and Pigott, 2005). Although the quantification of sediment removal during uplifts could not be calculated owing to the absence of estimates of intrabasinal palaeobathymety and to borehole-constrained reflection seismic profiles, preliminary modelling experiments demonstrated that realistic possible erosion magnitudes for this basin did not have a significant effect upon maturities.

Table 1. Maturity parameters obtained from previous studies (Harouna and Philp, 2012). Hopane isomerization = 22S/ (22S+22R) ratios, calculated on the C_{32} 17α (H)-homohopanes.

Well	Samples	Depth (m)	Tmax (°C)	Hop. Isom.
Yogou	HYU-1	2310	436	n.d
	HYU-2	2338	429	0.32
	HYU-3	2540	433	0.34
	HYU-4	2940	440	n.d
	HYU-5	2953	439	0.48
	HYU-6	2965	438	n.d
	HYU-7	2978	437	0.43
	HYU-8	3025	439	n.d
	HYU-9	3411	441	0.37
	HYU-10	3441	441	n.d
	HYU-11	3450	443	n.d
Sokor	HSK-1	1625	442	n.d
	HSK-2	1670	440	n.d
	HSK-3	1878	439	0.26
	HSK-4	2208	444	n.d
	HSK-5	2218	437	0.34
Goumeri	HGM-1	2155	442	n.d
	HGM-2	2205	440	0.24
	HGM-3	2280	441	n.d
	HGM-4	2298	440	0.24
	HGM-5	2335	444	0.28
	HGM-6	2405	442	0.36
	HGM-7	2415	443	n.d
	HGM-8	2555	441	0.41
	HGM-9	2815	440	n.d
	HGM-10	3048	440	0.28
	HGM-11	2384	442	n.d
Faringa	HFG-1	2160	443	0.22
	HFG-2	2224	441	n.d
	HFG-3	2320	442	0.33
	HFG-4	2343	444	0.31
	HFG-5	2368	442	n.d
	HFG-6	2390	442	0.31
	HFG-7	2803	443	n.d
	HFG-8	2875	444	0.3
	HFG-9	2885	443	n.d
	HFG-10	2895	443	0.28
Karam	HKR-1	1816	435	n.d
	HKR-2	2093	440	n.d
	HKR-3	2216	440	n.d
	HKR-4	2220	441	n.d
	HKR-5	2283	441	n.d
	HKR-6	2386	437	n.d
	HKR-7	2393	439	n.d
Boujamah	HBJ-3	1698	440	0.21
	HBJ-1	1932	439	0.16
	HBJ-2	1941	437	n.d
Sountellane	HST-1	1759	429	n.d
	HST-2	1776	427	n.d
Soudana	HSD-1	1258	426	n.d

Thermal Maturity

Three benchmarks were used for determining the level of thermal maturity in potential source rocks in the Termit Basin. First, kinetic thermal maturities of designated source rocks within the wells studied were calculated using the Lawrence Livermore National Laboratory programme (Sweeney *et al.*, 1990) within BasinMod. The second metric of thermal maturity was estimated from Rock-Eval T_{max} values. The oil window is generally assumed to be between T_{max} of 430 °C and 465 ° (Espitalié *et al.*, 1984); T_{max} values in the range 435-445 °C correspond to the early mature stage, and 445-450 °C and 450-470 °C to the mid- and late mature stages, respectively (Peters and Cassa, 1994). The third maturation index utilized was the hopane isomerization ratio at C_{22} (22S/22S + 22R). Initial oil generation occurs between ratio values of 0.50 and 0.55 (Seifert and Moldowan, 1986). An equilibrium value is reached at thepeak of oil generation at a ratio value of 0.6. These latter two maturity data i.e. Rock-Eval T_{max} and homohopane 22S/ (22S+22R) ratios are shown in Table 1.

RESULTS

Burial, tectonic subsidence and thermal history

The tectonic subsidence analysis of the Termit Basin boreholes provides insight into the timing and magnitude of non-topographic subsidence accompanying sediment deposition and the concomitant thermal changes. Similarities in the timing of tectonic subsidence pulses (tectonic subsidence and tectonic subsidence rate) exhibited by the borehole data corresponds to a convenient division of the Termit Basin into four regions (southern, central-west, northern and eastern, and western)

1. Southern Termit Basin: Well Yogou-1

Yogou-1 well was drilled in 1979 by Esso Exploration & Production Niger, Inc. in the southeast of the Termit Graben. Input data used to model this well are shown in Table 2. The well was drilled to a depth of 3998 m and bottomed in mid-Santonian limestones and shales. Three formation temperatures were obtained from the well-log completion report and, with a surface temperature of 23 °C, provide a current heat flow value of 40.24 mW/m^2.

Burial and thermal history profiles for the well are presented in Fig. 6. The tectonic subsidence curve (Fig. 6A) indicates rapid subsidence in the Late Cretaceous (85–75 Ma) followed by slower subsidence between 75 and 28 Ma (Maastrichtian to Paleogene). Beginning in the Late Oligocene (28 Ma) a phase of rapid subsidence was followed by slower subsidence which continues to the present dayThe modelled thermal evolution profile obtained using the present-day heat-flow is shown in Fig. 6B and shows a good match to measured Rock-Eval T_{max} values (see below). Tectonically, a steep gradient owing to fault mechanical subsidence indicates crustal extension or rifting, whereas a gentle gradient with a decreasing rate indicates thermal subsidence (Ru and Pigott, 1986).

2. Central West Termit Basin: Wells Sokor-1, Goumeri-1, and Karam-1

Well Sokor-1: The Sokor-1 well was drilled in 1982 by Elf Aquitaine in the central Termit Graben (Fig. 5). Input data used to model this well are given in Table 3. The well was drilled to a total depth of 2478 m, bottoming in sandstones of Maastrichtian to Paleocene age. The current heat flow value of 54.56 mW/m^2 was calculated from the two available formation temperatures with a surface temperature of 23°C. Burial and thermal history profiles for this well are presented in Fig. 7. The tectonic subsidence curve (Fig. 7A) shows the relative importance of Oligocene subsidence. The modelled thermal history profile obtained using a constant heat-flow is shown in Fig. 7B.

Well Goumeri-1: The Goumeri-1 well was drilled in 1990 by Elf Aquitaine in the central Termit Graben. Input data used to model the well are shown in Table 4. The well was drilled to a total depth of 3280 m, ending in Eocene sandstones. As formation temperatures were not provided in the well completion report, a heat flow value cannot be directly calculated. Burial and thermal history profiles for this well are presented in Fig. 8. The steep gradient of the tectonic subsidence curve (Fig. 8A) indicates a period of rapid subsidence during the Oligocene.

Figs 7A and 8A illustrate a remarkably similar history of tectonic subsidence and tectonic subsidence rate for the two western wells, Sokor-1 and Goumeri-1. The data suggest slow subsidence from the Late Cretaceous to the Paleocene (75–53 Ma), increasing subsidence rates during the Eocene (53–35 Ma) and then rapid subsidence (35–25 Ma) followed by slower subsidence from the Late Oligocene to the present day (25–0 Ma).

Well Karam-1: The Karam-1 well was drilled in 1994 by Elf Aquitaine. Input data used for this modelling is shown in Table 6. The well was drilled to a total depth of 2550 m, reaching shales of Paleocene age. Three formation temperatures were obtained from the well completion report. A current heat-flow value of 58.81 mW/m^2 was calculated from three formation temperatures and a surface temperature of 23 °C. Burial and thermal history profiles for this well are presented in Fig. 10. The tectonic subsidence curve (Fig. 10A) shows a phase of Oligocene subsidence. In contrast to

Table 2. Input data used for numerical modelling of the Yogou-1 well.

Formation	Age (Ma)	Lithology	Top (m)	Thick -ness (m)	Corrected Borehole Temp. (°C)	Heat Flow (mW/m^2)
Miocene-Recent	25.5	Sandstones/shales	0	738	23@0m	40.24
Oligocene	28.8	Shales	738	366		
Mid Oligocene	36	Sandstones	1104	251	68.58@ 1159 m	
Eocene	54	Shales/sandstones	1355	436		
L.Eoc. - Paleoc.						
Up.Maastrichtian	66.5	Sandstones/shales	1791	588		
Mid Maastr.	74-84	Sandstones/shales	2379	256		
Santonian		Shales	2635	388	94.22@ 2778 m	
Mid Santonian	84-88	Shales/limestones	3023	458		
Mid Coniacian		Shales	3481			
			TD @ 3998 m		151.12@ 3998 m	

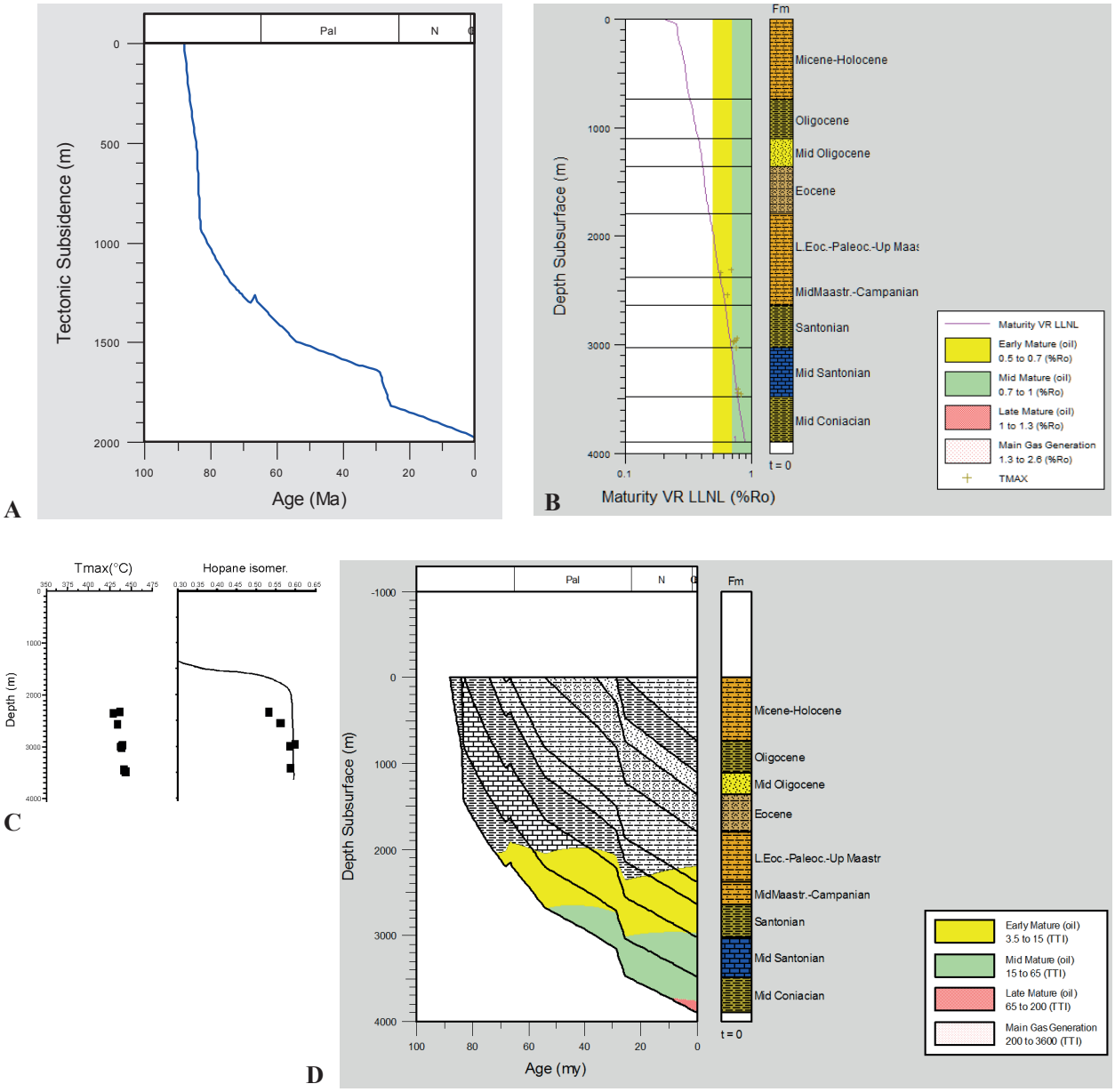

Fig. 6. Burial and thermal history profiles for the Yogou-1 well showing (A) the tectonic subsidence curve, where steep gradients represent rifting and gentle gradients represent thermal subsidence; (B) the modelled maturity curve for a present-day heat flow of 40.2 mW/m² (red line); (C) T_{max} values and hopane isomerization ratios versus depth; (D) the modelled hydrocarbon generation zones.

Table 3. Input data used for numerical modelling of the Sokor-1 well.

Formation	Age (Ma)	Lithology	Top (m)	Thick -ness (m)	Surf. Temp. (°C)	Borehole Temp. (°C)	Corrected Temp. (°C)	Heat Flow (mW/m_2)
Mioc.-Plio.	25.2	Sandstones	0	1050	23			
Oligocene	36	Shales	1050	600		48.8 @ 1055 m	56.5	50.7
Eocene	54	Shales/ sandstones	1650	585				
Paleoc.	74	Sandstones	2235					
			TD @ 2470 m			88.8 @ 2470 m	97.9	

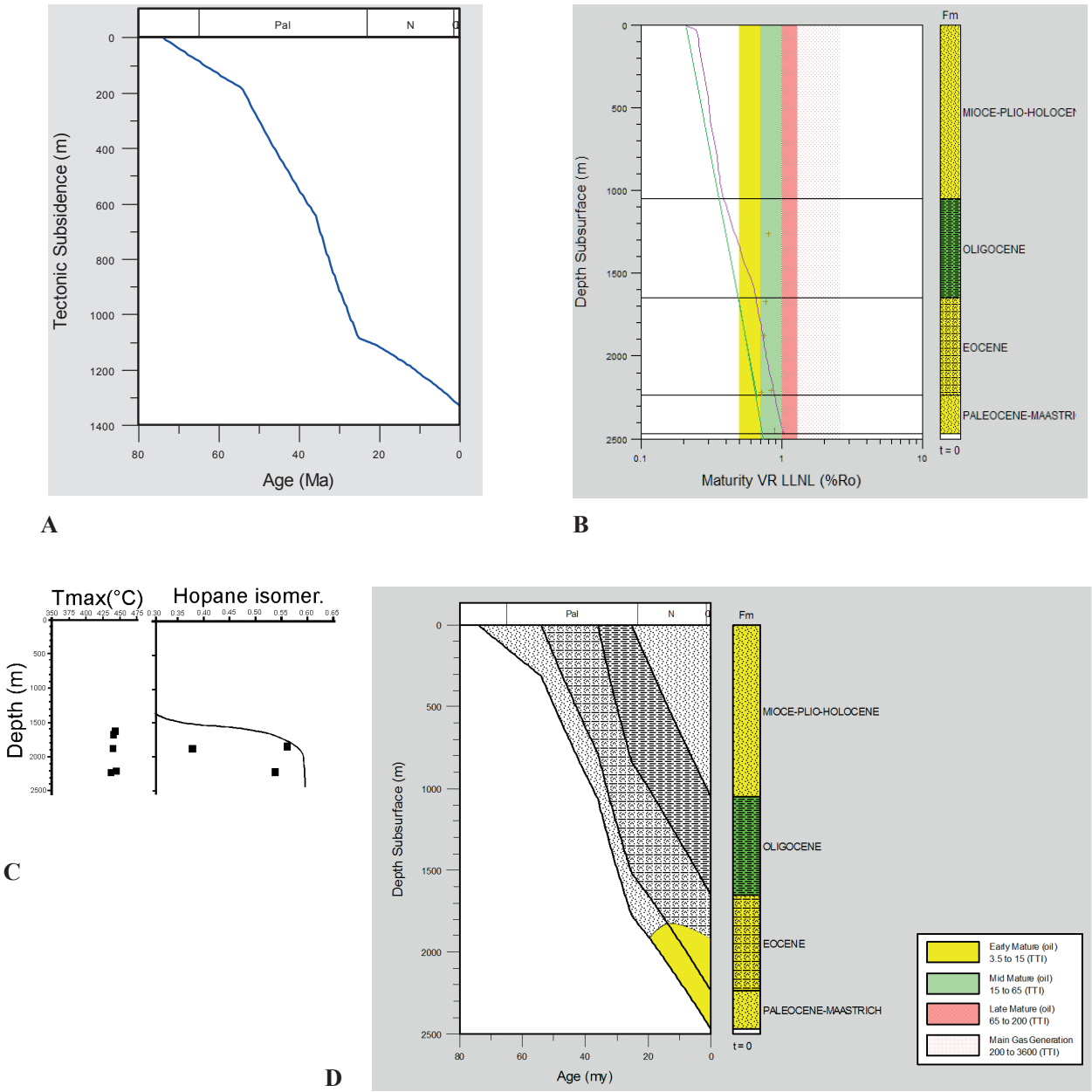

Fig. 7. Burial and thermal history profiles for the Sokor-1 well showing (A) the tectonic subsidence curve; (B) the modelled maturity curve for a present-day heat flow of 54.6 mW/m² (green line) and for an elevated heat flow of 80 mW/m² (red line); (C) T_{max} values and hopane isomerization ratios versus depth; (D) the modelled hydrocarbon generation zones.

the above two wells, during the Maastrichtian to early Paleocene (73–68 Ma), Karam-1 displays very rapid subsidence which slows slightly from the Paleocene to the Eocene (68 – 36 Ma). But similar to the two wells, a pulse of rapid tectonic subsidence occurs during the Oligocene (36–25 Ma) which then slows to the present (25–0 Ma).

3. Northern and Eastern Termit Basin

Well Sountellane-1: The Sountellane-1 well was drilled in 1998 by Esso Exploitation & Production Niger Inc. in the NE Termit Graben. Input data used for the modelling is given in Table 7. The well was drilled to a total depth of 2298 m, reaching sandstones of Maastrichtian to Paleocene age. Four formation temperatures were obtained from the well completion report. A heat flow value of 54.83 mW/m^2 is calculated from the four formation temperatures and a surface temperature of 23°C. The burial and thermal history profiles for the well are presented in Fig. 11. The tectonic subsidence curve (Fig. 11A) shows a relatively greater magnitude of Eocene to Oligocene and Recent subsidence. The thermal evolution profile obtained using constant current heat flow is shown in Fig. 11B.

Well Boujamah-1: The Boujamah-1 well was drilled in 1997 by Esso Exploitation & Production Niger Inc. in the central Termit Graben. Input data used for the modelling is given in Table 8. The well was drilled to a total depth of 2268 m, bottoming in sandstones of Maastrichtian to Paleocene age. Three formation temperatures were obtained from the completion report. A current heat flow value of 62.81 mW/m^2 was calculated from the three formation temperatures with a surface temperature of 23°C. The burial and thermal history profiles for this well are presented in Fig. 12. The tectonic subsidence curve (Fig. 12A) shows phases of Eocene to Oligocene and Recent subsidence. The thermal evolution profile obtained using constant current heat flow is shown in Fig. 12B.

Well Soudana-1: The Soudana-1 well was drilled in 1998 by Esso Exploitation & Production Niger Inc. in the NE Termit Graben. Input data are given in Table 9. The well was drilled to a total depth of 1448 m, reaching sandstones and shales of Maastrichtian to Paleocene age. Four formation temperatures were obtained from the completion report, and the current heat flow of 80.2 mW/m^2 was calculated with a surface temperature of 23°C. The burial and thermal history profiles for this well are presented in Fig. 13. The tectonic subsidence curve (Fig. 13A) shows phases of Eocene to Oligocene and Recent subsidence.

The tectonic subsidence observed at these three wells shares three similar pulses, although the magnitude of the tectonic subsidence rates at Soudana -1 is attenuated. Relatively rapid subsidence occurred from the Maastrichtian to the early Paleocene (73–68 Ma), followed by less rapid subsidence during the Paleocene to Early Eocene (68–52 Ma), and then a phase of more rapid subsidence from the Early Eocene to the Late Oligocene (52 –25 Ma). Tectonic subsidence slows during the Late Oligocene and Miocene (25 –5 Ma), ending with a more rapid subsidence phase from the Pliocene to the present day (5–0 Ma).

4. Western Termit Basin

Well Faringa-1: The Faringa-1 well was drilled in 1993 by Elf Aquitaine in the central Termit Graben. Input data used for modelling the well are given in Table 5. The well was drilled to a total depth of 3120 m bottoming in Eocene sandstones. In the absence of formation temperatures, a heat flow value cannot be directly calculated. The burial and thermal history profiles for this well are presented in Fig. 9. This borehole shares only one major tectonic pulse with the other boreholes, that of the Late Oligoene. A tectonic subsidence curve for well Faringa-1 is shown in Fig. 9A. Slow tectonic subsidence was recorded from the Maastrichtian to the early Paleocene (73–68 Ma) with a slightly increased rate from the Paleocene to the Eocene (68–28 Ma). A rapid pulse occurs in the Late Oligocene (28–25 Ma) which then slows to the present (25–0 Ma).

DISCUSSION

Termit Basin Tectonics

While the observed pulses of tectonic subsidence indicative of crustal extension within the Termit Basin boreholes vary in magnitude, rate and timing, within the four groups of wells there are coeval pulses of activity. Although it is not clear if the shared tectonic pulses of the four groups imply a connected crustal platform, most but not all of the boreholes share the episodes and some show additional uncorrelated times of rapid tectonic subsidence. Such variations in tectonic subsidence, even within the same basin entity, is to be expected within this transtensional graben (Genik, 1993). For example, the natural curvilinear nature of through-going strike-slip faults in which releasing fault bends with accelerating subsidence can evolve into constraining fault bends with diminished to even reversals in subsidence and vice versa has been demonstrated elsewhere in similar basins (Christie-Blick and Biddle, 1985; Ru and Pigott, 1985; Pigott and Sattayarak, 1993). Perhaps those borehole groups which share tectonic events are located along connecting master faults, and those that do not represent separate basin segments. Without seismic reflection data to confirm this, however, the connectivity is only speculative.

Table 4. Input data used for numerical modelling of the Goumeri-1 well.

Formation	Age (Ma)	Lithology	Top (m)	Thickness (m)	Heat Flow (mW/m^2)
Mioc.-Plio.	25.2	Sandstones	0	1465	58.6
Oligocene	36	Shales	1465	815	
Eocene	54	Shales/sandstones	2280	895	
Paleoc.-Maastrichtian	74	Sandstones	3175		*BASIN AVERAGE
			TD @ 3280 m		

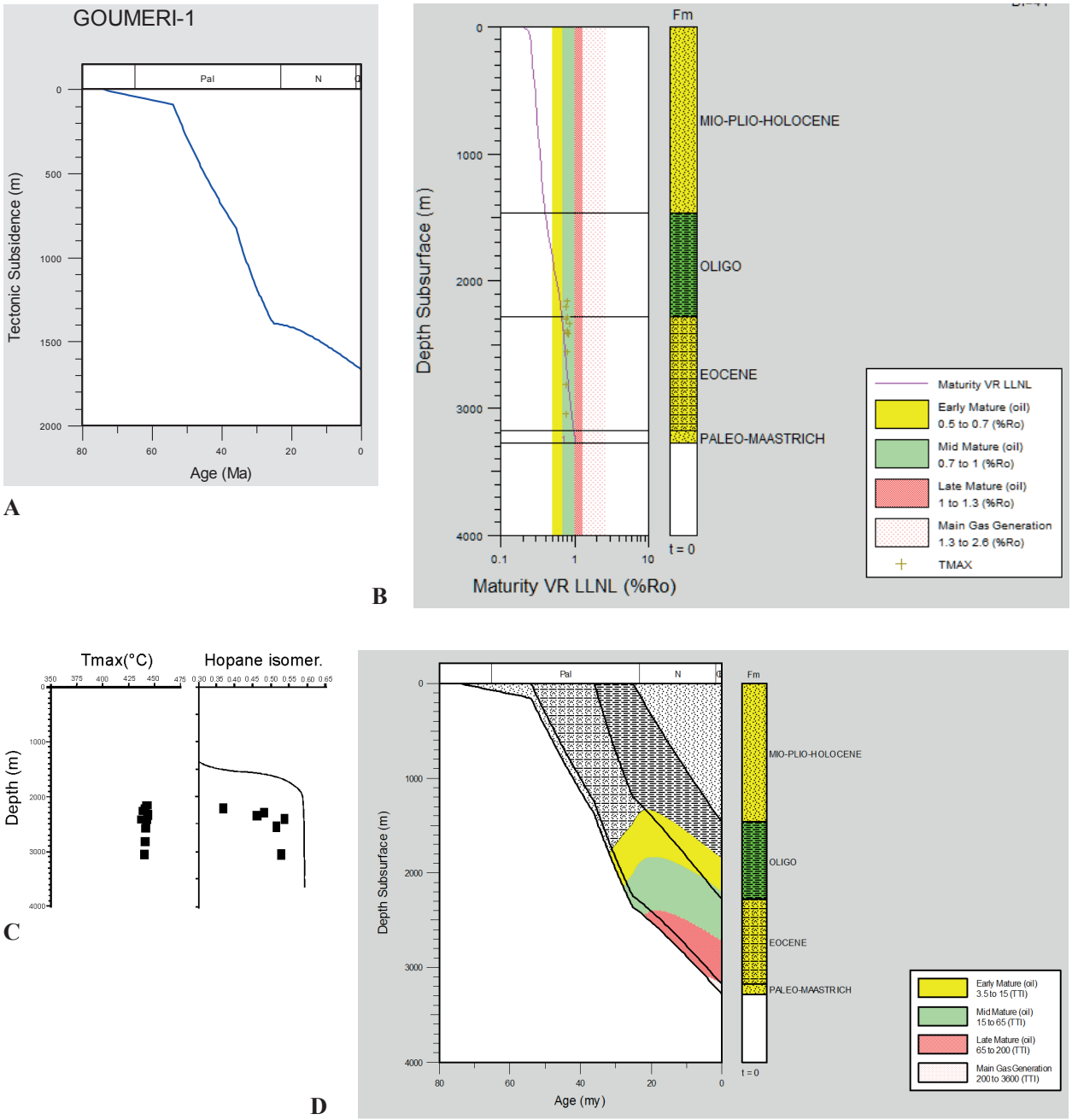

Fig. 8. Burial and thermal history profiles for the Goumeri-1 well showing (A) the tectonic subsidence curve; (B) the modelled maturity curve for a present-day basin average heat flow of 58.6 mW/m^2 (red line); (C) T_{max} values and hopane isomerization ratios versus depth; (D) the modelled hydrocarbon generation zones.

Table 5. Input data used for numerical modelling of the Faringa-1 well.

Formation	Age (Ma)	Lithology	Top (m)	Thickness (m)	Heat Flow (mW/m^2)
Mioc.-Plioc.	25.2	Sandstones	0	1551	58.6 mW/m^2
Late Oligocene	28.8	Shales	1551	398	
Early Oligocene	36	Shales/sandstones	1949	276	
Eocene	54	Shales/sandstones	2225	570	*BASIN AVERAGE
Paleocene	66.5	Shales	2795	222	
Paleoc.	74	Sandstones	3017		
			TD @ 3120 m		

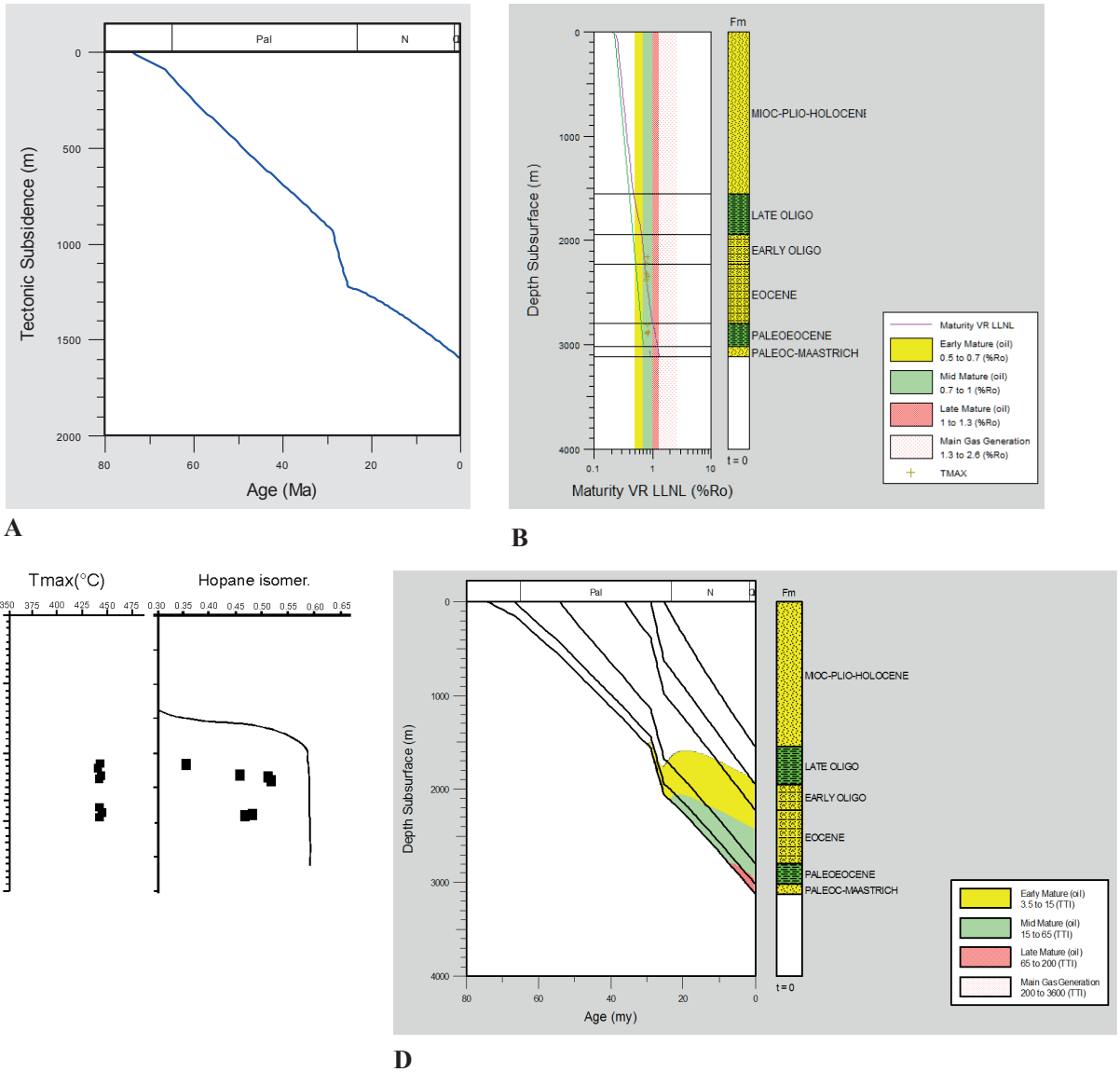

Fig. 9. Burial and thermal history profiles for the Faringa-1 well showing (A) the tectonic subsidence curve; (B) the modelled maturity curve for a present-day basin average heat flow of 58.6 mW/m^2 (green line) and for an elevated heat flow of 80 mW/m^2 (red line); (C) T_{max} values and hopane isomerization ratios versus depth; (D) the modelled hydrocarbon generation zones.

Table 6. Input data used for numerical modelling of the Karam-1 well.

Formation	Age (Ma)	Lithology	Top (m)	Thick -ness (m)	Surf. Temp. (°C)	Borehole Temp. (°C)	Corrected Temp. (°C)	Heat Flow (mW/m^2)
Mioc.-Plioc.	25.2	Sandstones	0	839	23			58.8
Late Oligocene	28.8	Shales	839	211				
Early Oligocene	36	Shales/sandstones	1050	484				
Eocene	54	Shales/sandstones	1534	636		78 @ 1816 m	86.7	
Paleocene	66.5	Shales	2170	232		88.2 @ 2169.7 m	97.3	
Paleoc.	74	Sandstones	2402			98.3 @ 2410.5 m	108.7	
			TD @ 3998 m					

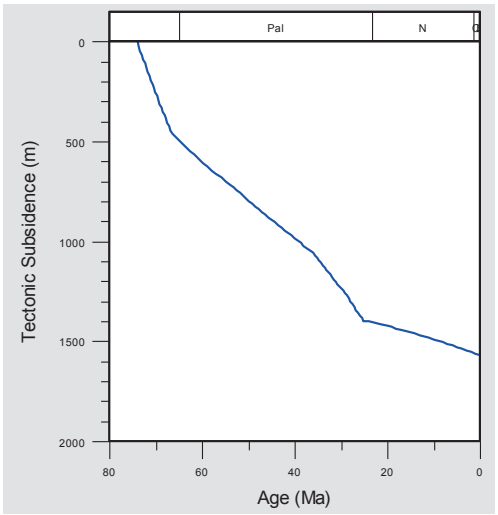

A

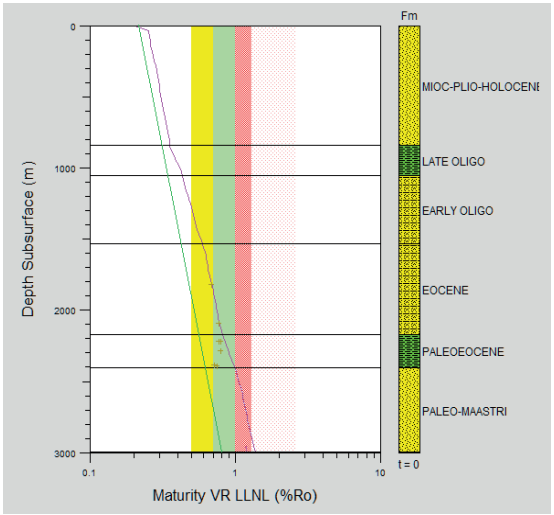

B

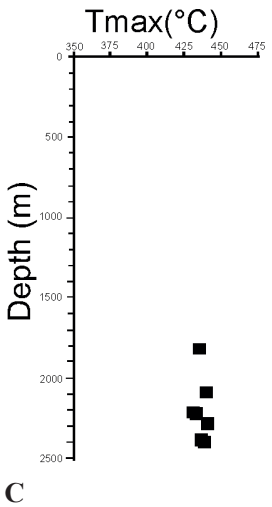

C

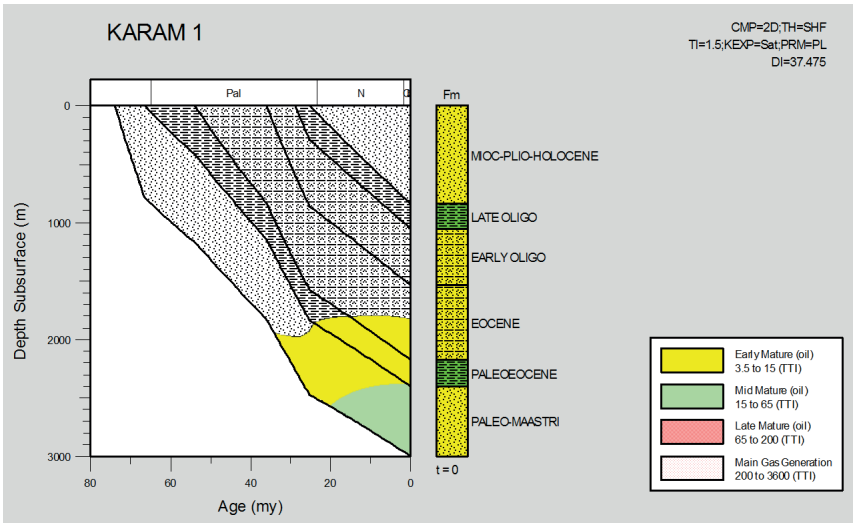

D

Fig. 10. Burial and thermal history profiles for the Karam-1 well showing (A) the tectonic subsidence curve; (B) the modelled maturity curve for a present-day heat flow of 58.8 mW/m^2 (green line) and for an elevated heat flow of 80 mW/m^2 (red line); (C) T_{max} values versus depth; (D) the modelled hydrocarbon generation zones.

Table 7. Input data used for numerical modelling of the Sountellane-1 well.

Formation	Age (Ma)	Lithology	Top (m)	Thickness (m)	Surf. Temp. (°C)	Borehole Temp. (°C)	Corrected Temp.(°C)	Heat Flow (mW/m^2)
Late Mioc.	5.2	Sandstones	0	466	23			54.8
Early Miocene	25.2	Shales	466	285				
Oligocene	36	Shales/sandstones	751	452(fault)		50.9 @ 740 m	58.6	
Eocene	54	Sandstones/shales	1203	673		60.1 @ 1209 m	68.2	
Paleocene	66.5	Sandstones	1876	183		80.3 @ 1889 m	89.1	
Paleoc.	74	Sandstones	2059			81.1 @ 2006 m	89.9	
			TD @ 2298 m					

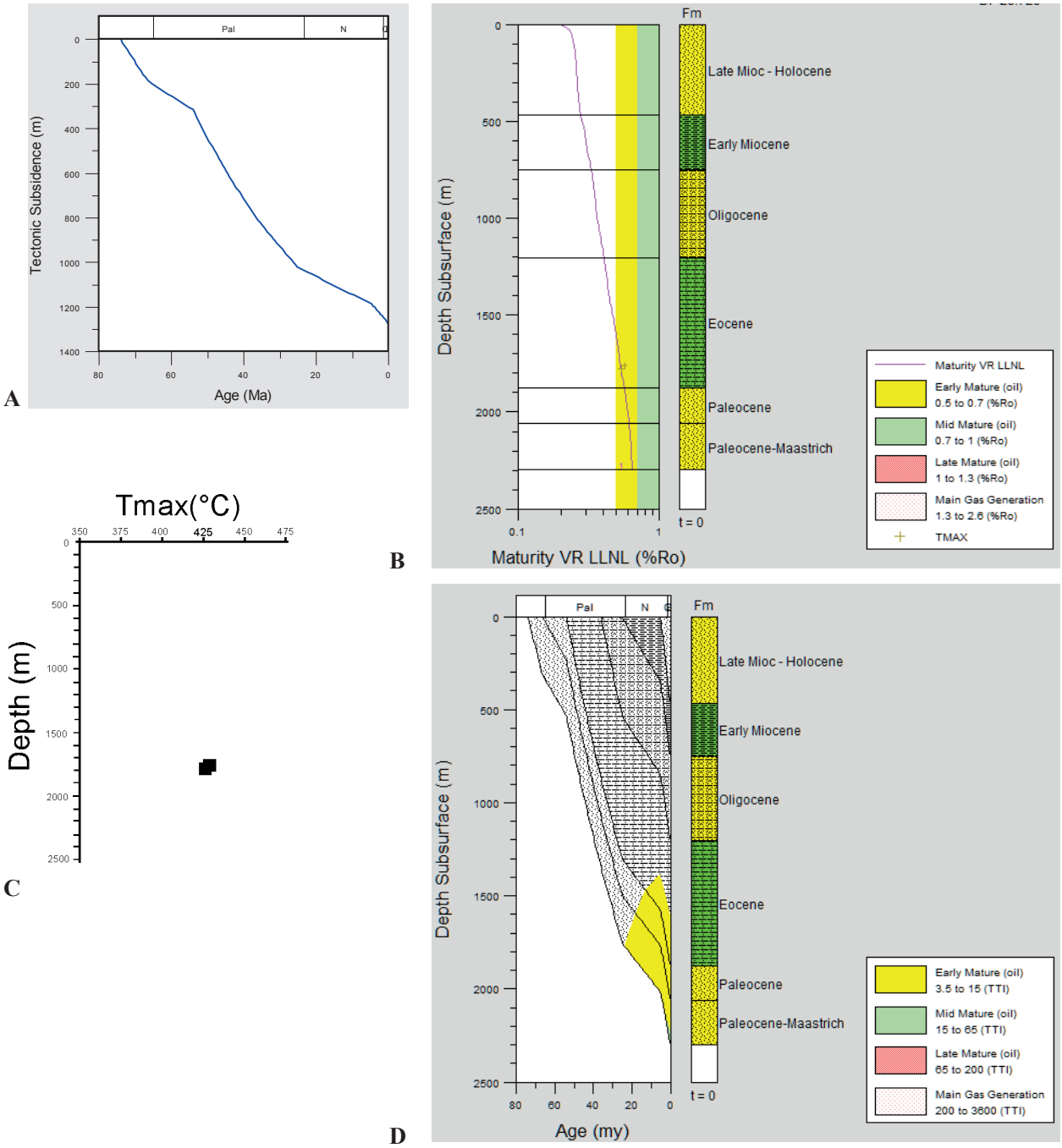

Fig. 11. Burial and thermal history profiles for the Sountellane-1 well showing (A) the tectonic subsidence curve; (B) the modelled maturity curve for a present-day heat flow of 54.8 mW/m^2 (red line); (C) T_{max} values versus depth; (D) the modelled hydrocarbon generation zones.

Table 8. Input data used for numerical modelling of the Boujamah-1 well.

Formation	Age (ma)	Lithology	Top (m)	Thick-ness (m)	Surf. Temp. (°C)	Borehole Temp. (°C)	Corrected Temp. (°C)	Heat Flow (mW/m^2)
Late Mioc.	5.2	Sandstones	0	440	23			62.8
Early Miocene	25.2	Shales/sandstones	440	447				
Late Oligocene	28.8	Shales	887	186				
Early Oligocene	36	Shales	1073	226				
Eocene	54	Shales/sandstones	1299	560		67.9 @ 1300 m	76.2	
Paleocene	66.5	Sandstones/shales	1859	177		95.6 @ 1969 m	104.9	
Paleoc.	74	Sandstones	2036			99.42 @ 2031 m	108.9	
			TD @ 2268 m					

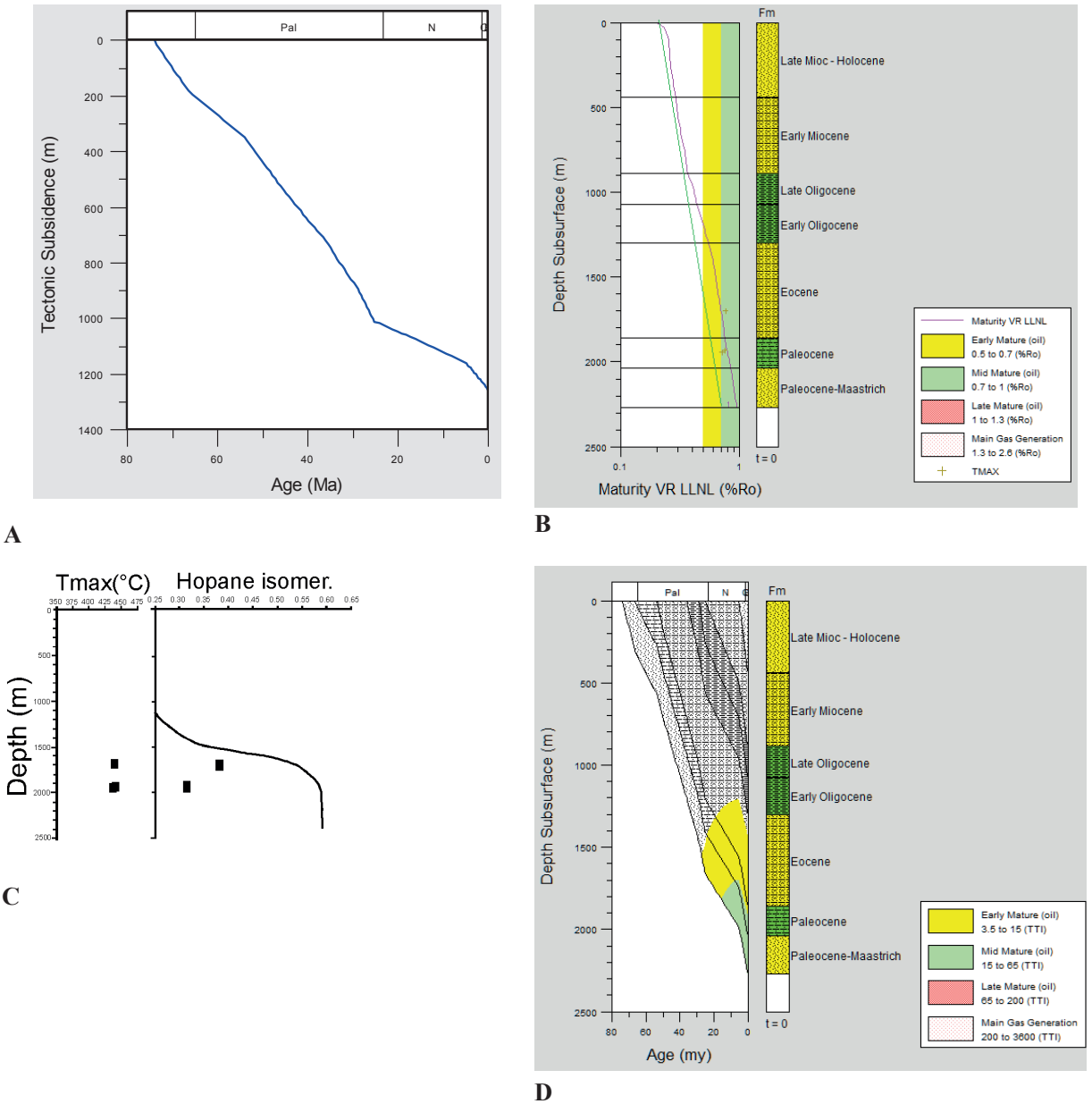

Fig. 12. Burial and thermal history profiles for the Boujamah-1 well showing (A) the tectonic subsidence curve; (B) the modelled maturity curve for a present-day heat flow of 62.8 mW/m² (green line) and for an elevated heat flow of 80 mW/m2 (red line); (C) T_{max} values and hopane isomerization ratios evolution versus depth; (D) the modelled hydrocarbon generation zones.

There are three episodes of observed rapid tectonic subsidence (>50m/Ma) within the basin which correspond to the three previously-mentioned fault-mechanical episodes: Episode 1, syn-Cretaceous (recorded only by the deepest borehole, Yougou-1); Episode 2, Maastrichtian to Early Paleocene; and Episode 3, Oligocene. In general, between and following these three episodes were times of less rapid tectonic subsidence.

These three episodes of crustal extension lie within the regional tectonic phases for the West African rift system identified by Genik (1993). Episode 1 corresponds to Late Cretaceous rifting during Genik's Tectonic Phase 2. Episode 2, the phase of rapid subsidence in the Maastrichtian to early Paleocene correlates with Genik's (*ibid.*) Tectonic Phase 3, a rift phase in the West and Central Africa Rift System. The following phase of reduced tectonic subsidence in the Termit Basin corresponds to Genik's Tectonic Phase 4, a time of regionally slow rift activity. The observed Termit Basin phase of rapid tectonic subsidence in the Oligocene (Episode 3) occurs at the end of Genik's (*ibid.*) Phase 4, when another rift cycle developed in the West African and Central African rifts. Consistent with Genik's final Tectonic Phase 5, a period of regional uplift and emergence continuing to the present day, the Termit Basin boreholes in general show minor tectonic subsidence except for a few local anomalies.

LEVELS OF ORGANIC MATURITY

Regional grouping of boreholes

1. Southern Termit: Well Yogou-1

For this well (Fig. 6B), the thermal kinetic model using present-day heat flow values of 40.2 mW/m^2 lies only slightly below the measured T_{max} data (Fig. 6C). Plots of T_{max} values and hopane isomerization ratios from Harouna and Philp (2012) versus depth are given in Fig. 6C. The T_{max} data is from the Maastrichtian-Campanian and Santonian sequences between depths of 2300 and 3500 m, with low S_2 values (Harouna and Philp, 2012). Modelled hydrocarbon generation zones are shown on Fig. 6D. The Early Mature zone occurs at a depth of about 2200 m, and the Mid Mature zone between 3300 and 3500 m. Hopane isomerization values reach the oil window at 2250 m and approach equilibrium values at around 3000 m (Fig. 6C).

The maturity profile (Fig. 6D) indicates that the Early Mature stage was reached by the Mid Coniacian interval at about 71 Ma, by the Mid Santonian around 58 Ma, by the Upper Santonian at 40 Ma, and by the Mid Maastrichtian to Campanian and Upper Campanian – Paleocene – Lower Eocene at about 15 Ma and 8 Ma, respectively. The Mid Coniacian entered the Mid Mature zone at about 52 Ma, while the Mid Santonian entered the same zone around 25 Ma. Only the Mid Coniacian interval reached the Late Mature stage, at about 8 Ma. Organic matter corresponds to Type III kerogen (Harouna and Philp, 2012).

2. Central West Termit:
Wells Sokor-1, Goumeri-1, and Karam-1

Well Sokor-1: Thermal modelling of well Sokor-1 using a present-day heat flow of 54.6 mW/m^2 (Fig. 7B) provides a less satisfactory match between the modelled profile and the measured T_{max} values. Profiles of T_{max} and homohopane isomerization ratios are plotted versus depth in Fig. 7C; all the T_{max} data are in the Oligocene and Eocene interval between 1500 and 2250 m. Modelled hydrocarbon generation zones are shown in Fig. 7D. While the T_{max} evolution (Fig. 7C) reached the early mature stage at a depth of about 1600 m, the hopane isomerization values correlate with the beginning of the oil window over 2000 m (Fig. 7C), indicating that there is disagreement between the two maturity parameters. The maturity profile (Fig. 7D) indicates that the Paleocene to Maastrichtian and the Eocene entered the oil window at about 20 Ma and 12 Ma, respectively. Modelling demonstrates that, only if the present-day heat flow were elevated to approximately 80 mW/m^2 would the kinetic model match that observed geochemical maturity values, implying that this portion of the graben has been cooling considerably since the original phase of crustal stretching.

Well Gourmeri-1: The Goumeri-1 well lacks borehole temperature data. A present-day assumed heat flow of 58.6 mW/m^2 (the average heat flow of all the Termit Basin values) indicates a satisfactory match between the profile obtained by modelling and the measured T_{max} values. The thermal evolution profile obtained using this heat-flow is shown in Fig. 8B, and plots of T_{max} values and homohopane isomerization ratios versus depth are given in Fig. 8C. The T_{max} data are taken from the Oligocene and Eocene succession between 2200 and 3100 m. Modelled hydrocarbon generation zones are shown in Fig. 8D. However, T_{max} data (Fig. 8C) in the Oligocene and Eocene indicated that all the studied samples are Early Mature which does not agree with the hopane isomerization values which indicate that the early mature stage is reached below about 2300 m. Based on the maturity profile (Fig. 8D), the Paleocene to Maastrichtian interval entered the oil window at 32 Ma, the mid-mature zone at 27 Ma, the Late Mature zone at 22 Ma and the main gas generation stage at 4 Ma. The Eocene entered the oil window at 30 Ma, the mid-mature zone at 25 Ma, and the Late Mature zone at 20 Ma. The Oligocene entered the oil window at 20 Ma and the mid-mature stage at 2 Ma.

Table 9. Input data used for numerical modelling of the Soudana-1 well.

Formation	Age (Ma)	Lithology	Top (m)	Thick -ness (m)	Surf. Temp. (°C)	Borehole Temp. (°C)	Corrected Temp. (°C)	Heat Flow (mW/m^2)
Late Mioc.	5.2	Sandstones	0.0	333.0		23@0m		80.2
Early Miocene	25.2	Sandstones	333.0	188.0				
Late Oligocene	28.8	Shales	521.0	82.0				
Early Oligocene	36.0	Shales/sandstones	603.0	207.0		56.3@ 603 m	64.2	
Eocene	54.0	Sandstones	810.0	364.0		55.3@ 788 m	63.2	
Paleocene	66.5	Sandstones	1174.0	158.0		62.7@ 1153 m	70.9	
Paleoc.-	74.0	Sandstones/shales	1332.0			65.3@ 1357 m	73.6	
			TD @ 1448 m					

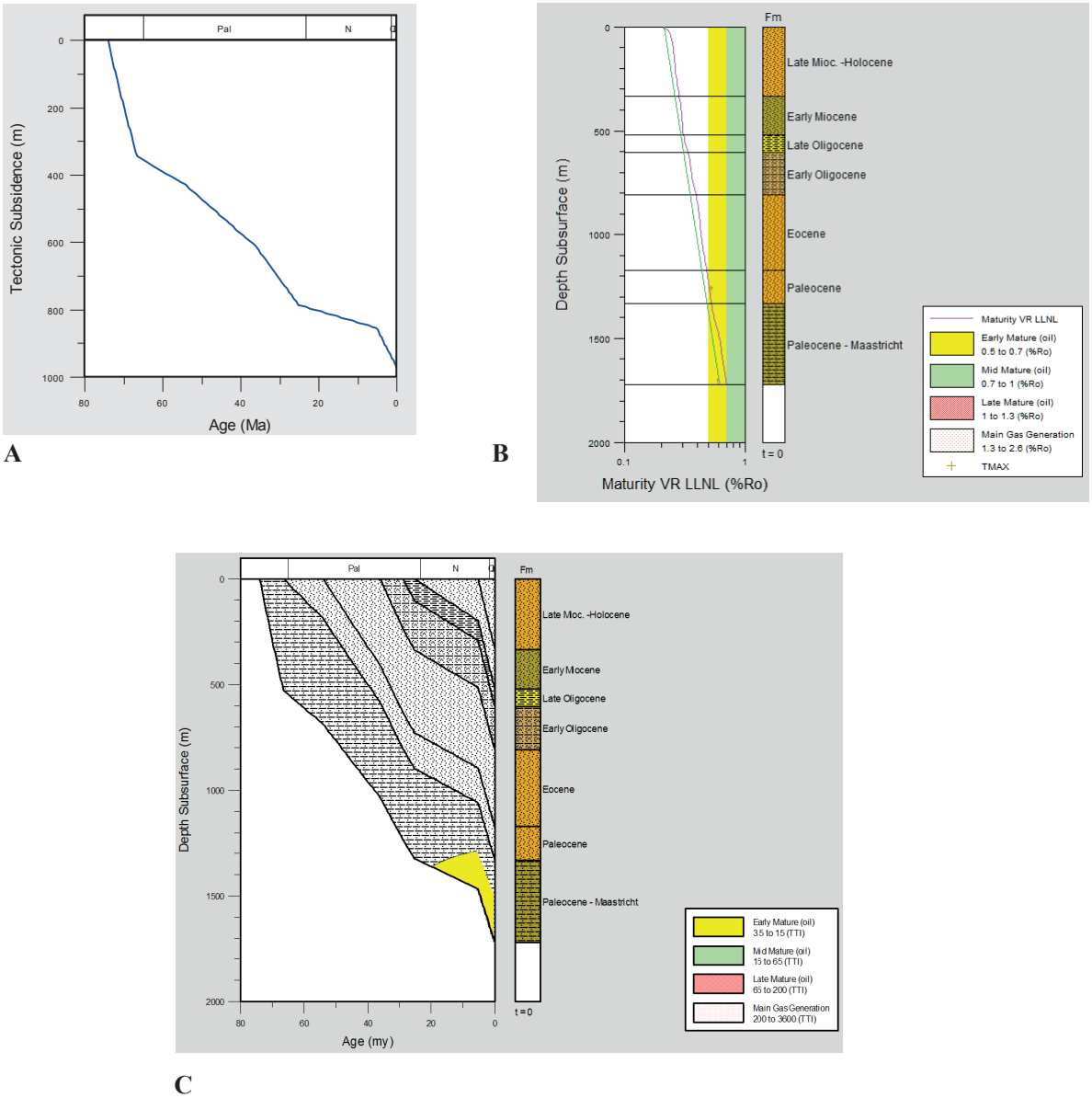

Fig. 13. Burial and thermal history profiles for the Soudana-1 well showing (A) the tectonic subsidence curve; (B) the modelled maturity curve for a present-day heat flow of 80.2 mW/m²(green line) and for an elevated heat flow of 90 mW/m² (red line); and (C) the modelled hydrocarbon generation zones.

Well Karam-1 Thermal modelling of well Karam-1 using the present-day heat flow of 58.8 mW/m^2 (Fig. 10B) suggests that the modelled profile underestimates the measured T_{max} data. The thermal evolution profile obtained using constant present-day heat-flow is shown in Fig.10B. A plot of T_{max} values versus depth is shown in Fig. 10C; the T_{max} data are in the Eocene and Paleocene succession between 1800 and 2400 m. Modelled hydrocarbon generation zones are shown in Fig. 10D.

Most of the T_{max} values, between 1800 and 2400 m ranging from 435 to 443 °C, have reached the onset of the oil window (Fig. 10C). The Lower Paleocene – Maastrichtian reached the Early Mature and Mid Mature zones at 34 Ma and 20 Ma, respectively. The Paleocene and the Eocene entered the oil window at about 25 and 18 Ma, respectively (Fig. 10D).

3. Northern and Eastern Termit:
Wells Soutenallane-1, Boujaman-1, and Soudana-1

Well Sountellane-1: Fig. 11B illustrates thermal modelling of the Sountellane-1 well, using the present-day heat flow of 54.8 mW/m^2. Only two T_{max} values of 429 and 427 °C at 1759 and 1776 m depth were available (Fig. 11C) and were obtained in the Eocene sequence between 1750 and 1800 m (Fig. 11C). Modelled hydrocarbon generation zones are shown in Fig. 11D. The kinectic maturity curve slightly underestimates the T_{max} values (Fig. 11B). Based on the maturity profile (Fig. 11D), the Lower Paleocene – Maastrichtian and the Paleocene reached the Early Mature zone at about 24 Ma and 19 Ma, respectively.

Well Boujamah-1: Fig. 12B represents the thermal modelling of the Boujamah-1 well. Three T_{max} values were obtained in the Eocene and Paleocene strata between 1600 and 1900 m, and hopane isomerization ratios are given in Fig. 12C. Modelled hydrocarbon generation zones are shown in Fig. 12D. The thermal modelling curve with a heat flow value of 62.8 mW/m^2 underestimates the measured T_{max} values ranging from 437 to 440 °C (Fig. 12C). Hopane isomerization values indicate that the samples are immature (Fig. 12C). The maturity profile (Fig. 12D) shows that the Early Paleocene – Maastrichtian interval entered the oil window and the Mid Mature stage at 25 Ma and 3 Ma, respectively. The Paleocene reached the Early Mature stage at 20 Ma and the Eocene at about 12 Ma.

Well Soudana-1: The thermal modelling of well Soudana-1 using the present-day heat flow of 80.2 mW/m^2 is illustrated in Fig. 13B. One T_{max} value is obtained from the Paleocene strata at 1258 m. Modelled hydrocarbon generation zones are shown in Fig. 13C. With only one T_{max} value of 426 °C available for this well, it is challenging to evaluate the significance with which the kinetic maturity profile misses the T_{max} value, as an increase to 90 mW/m^2 would be necessary. The calculated maturity profile (Fig. 13C) shows that the Lower Paleocene – Maastrichtian entered the Early Mature zone at 21 Ma.

4. Western Termit. Well Faringa-1
As Faringa-1 also lacks thermal borehole measurements, Fig. 9B illustrates the thermal model of well Faringa-1 using the present-day Termit average heat flow of 58.6 mW/m^2. The kinetic model line lies substantially below the measured T_{max} values, and there is no fit unless the heat flow is increased to 80 mW/m^2. The thermal evolution profile obtained using this heat-flow is shown in Fig. 9B, and plots of T_{max} values and homohopane isomerization ratios versus depth are given in Fig. 9C; the T_{max} data are in the Oligocene, Eocene and Paleocene sequences between 2000 and 3000 m. Modelled hydrocarbon generation zones are shown in Fig. 9D. Fig. 9C shows the evolution of T_{max} values versus depth for Faringa-1 samples from the Oligocene, Eocene and Paleocene. The T_{max} values show that all the samples have reached the Early Mature zone. Hopane isomerization values indicate that the Early Mature stage was reached at depths of over 2300 m (Fig. 9C), in disagreement with the maturity results given by the T_{max} values. The modelled maturity profile (Fig. 9D) shows that the Lower Paleocene and Maastrichtian entered the Early Mature, Mid Mature and Late Mature Stages at 30 Ma, 23 Ma and 8 Ma, respectively. The Paleocene reached the Early Mature and the Mid Mature Stages at 25 Ma and 20 Ma, respectively. The Eocene and the Early Oligocene entered the oil window at 22 Ma and 10 Ma, respectively.

DISCUSSION

Irrespective of the substantial heterogeneity exhibited throughout the Termit Basin, stratal groupings are largely consistent with respect to the kinetic modelled maturities. Grouped in increasing thermal maturity are the Oligocene, Paleocene, Maastrichtian-Campanian, and Santonian sources. Specifically, the Oligocene samples are largely thermally immature and only about one-half of them exhibit a thermal maturity level corresponding to the onset of the oil window (%R_o = 0.5). Most of Paleocene samples are also thermally immature whereas the Maastrichtian-Campanian samples are in general thermally mature with some reaching the main phase of oil generation (%R_o = 0.7). Finally, the thermal maturity of Santonian source rocks corresponds to an interval between the onset of the oil window and the main oil generation phase (%R_o = 0.7 to 1).

Regarding the significance of the timing of the fault mechanical stratigraphy (Figs 3 and 4), the differing times and degrees of maturation would directly affect hydrocarbon exploration strategies in the Termit Basin. If vertical intra-fault permeability is substantially higher than lateral cross-fault permeability, then the geomechanical elastic behavior of the basin fill owing to brittle failure of the rocks would lead to potential vertical (short distance) migration pathways. Moreover, as multiple source rocks would be juxtaposed next to the high angle faults, reservoir rock assemblages supplied by deeper source rocks would show less oil mixing than shallower ones. For example, the Termit Basin Santonian source rocks which matured earlier than the rest would potentially source those reservoir units which were connected via faults which developed in the Late Cretaceous. However, if the Santonian source pods were penetrated by faults of the Maastrichtian to early Paleocene and/or Oligocene, the petroleum fluids accumulating in shallower reservoirs would tend to be more mature (higher API, more gas) than if these same reservoirs were connected to shallower and later maturing source rocks. Such a contrast in sourced oil compositions would be revealed by Maastrichtian Campanian mature source rocks if directly connected to syndepositional and younger reservoirs.

For the studied wells, the T_{max} values in many cases are consistently higher than the modelled maturities. Discrepancies between the kinetic model and the T_{max} values may have a number of causes, e.g. systematic error in the calculations or error in the T_{max} values themselves. That the error could be due to the kinetic parameters used within the LLNL (Lawrence Livermore Nuclear Laboratory) programme utilized in BasinMod is considered unlikely as the Lawrence Livermore kinetics are rigorous and form a basin-modelling industry standard (see Burnham *et al.,* 1992). Then, could the surface temperatures used for the kinetic models be in error? Although the temperatures were corrected, the addition of more borehole temperatures and circulation times and/or drill stem tests definitely would greatly improve the accuracy of the thermal calculations. However, experiments for these wells show that unless the surface temperatures measures were more than 25% undervalued (which is unlikely), they are not in substantial error. Could the T_{max} values be in error? Rock-Eval T_{max} is the temperature which coincides with the maximum S_2 peak during anhydrous pyrolysis, and T_{max} values increase with thermal maturation (Espitalié *et al.*, 1984; Peters, 1986; Tissot *et al.*, 1987). Consequently T_{max} values can be, and are commonly, correlated with vitrinite reflectance values for Type III organic matter, including humic coals (Teichmüller and Durand, 1983; Espitalié *et al.*, 1984; Tissot and Welte, 1984; Waples, 1985). However, factors which may corrupt T_{max} profiles include contamination by drilling mud additives, the presence (and possible recycling) of bitumen, the organic matter type, the mineral matrix and mixing of reworked sedimentary materials (Kruge, 1983; Vandenbroucke *et al.*, 1983; Tissot and Welte, 1984; Peters, 1986; Hunt, 1996; Lee and Sun, 2014). But if such contamination were the case, the error would be likely random among the wells and not show an observed systematic maturity higher than that modelled.

Another discrepancy is that while T_{max} is in general a good indicator of thermal maturity, T_{max} values in the studied wells did not agree with hopane isomerization values which correlate with the other molecular maturity parameters (Harouna and Philp, 2012). For example, the T_{max} values obtained on Yogou-1 samples with very low S_2 peaks (Harouna and Philp, 2012) may be considered to be unreliable as well as the small number of values obtained from wells Sountellane-1 and Soudana-1 (two and one, respectively) were insufficient to show a consistent maturity trend. But, the hopane isomerization data-set may contain errors. For example, Rullkotter and Marzi (1988) proposed that the poor agreement (and therefore resulting errors) between hopane isomerization and other kinetic parameters are a result of the differences between the reactions in the laboratory and those theorized to occur in nature. Unfortunately, there are no measured vitrinite reflectance values to rigorously test either the hopane isomerization or T_{max} values.

If the geological, geophysical and geochemical data (especially the abundant T_{max} values) are accurate, there remains an additional possibility for the observed differences. With inputs from the tectonic subsidence parameters and using present-day heat flows, as mentioned previously the calculated maturity curves are in several instances under-mature with respect to the observed T_{max} values. That is, If both the T_{max} and temperature measurements are accurate, then there are in general two ways to shift the calculated kinetic maturity curve to the right: either geologically (i.e. by lithologic replacement); or tectonically, by thermal maturity models as discussed by Pigott and Abouelresh (2016).

For example, if the observed lithology conductivities were to be replaced (conductivity lithology replacement model procedure of Pigott *et al.*, 2008) with "all shale", the decrease in thermal conductivities would correspond to increased maturities and move the calculated curves to the right and closer to the T_{max} values. However, this assumption is not consistent with the multiple observations of sandstones logged in the wells. Tectonically, in the general crustal rifting model (Ru and Pigott, 1986), lithospheric thinning is accompanied by a heat pulse which decays over time. Heat flow modelling experiments with

Sokor-1, Faringa-1, Karam-1 and Boujamah-1 clearly demonstrate that if the synrift heat flow were elevated to 80 mW/m^2 from the present-day values, the kinetic maturities would fit the T_{max} values much better (see red lines on Figs. 7B, 9B, 10B and 12B which show the higher modelled maturities if the borehole heatflows are increased to 80 mW/m^2). A heat flow increase of such a magnitude would involve continental crust with an average heat flow of 65 Mw/m^2 and a beta (stretching) factor of 1.23, which approximates the stretching geometrically proposed by Genik's (1992) estimate of extension from 150 to 200 km (which results in a beta of 1.33). Moreover, such an increase in synrift palaeo-heat flows at values similar to the present-day value at Soudana -1, which later decayed to the present-day values, would reconcile the difference between the T_{max} and the kinetics.

CONCLUSIONS

Three episodes of tectonic subsidence indicative of crustal extension which correspond to the observed fault mechanical stratigraphy within the Termit Basin are identified in this study: Late Cretaceous, Maastrichtian to early Paleocene, and Oligocene. These episodes fall within the regional tectonic phases for the West African Rift System delineated by Genik (1992). The Termit Basin exhibits substantial heterogeneity in the magnitude of tectonic episodes and consequently in thermal maturities.

The thermal modelling suggests that most Oligocene source rocks are immature except in the Goumeri-1 and Faringa-1 wells, where they are mid-mature and early mature respectively. Eocene source rocks are immature in the Sountellane-1 and Soudana-1 wells; however, they have reached the early mature stage in Yogou-1, Sokor-1, Karam-1 and Boujamah-1, mid mature in Faringa-1, and late mature in Goumeri-1. Paleocene source rocks are immature in Soudana-1 but have entered in the early mature phase in Karam-1, Sountellane-1 and Boujamah-1. The mid mature stage was reached by Paleocene source rocks at the Faringa-1 well. All source rocks from the Lower Paleocene – Upper Maastrichtian interval are mature and have entered the mid mature stage in Boujamah-1 well, the late mature stage in Faringa-1, and have reached the main gas generation phase in the Goumeri-1 well. At Yogou-1, while Maastrichtian, Campanian and Santonian source rocks are early mature, the mid Santonian and mid Coniacian source rocks are mid mature and late mature, respectively.

Kinetic modelling of maturities fits the T_{max} values of those wells which either have high present-day heat flows or inferred elevated heat flows in the past owing to a beta value of 1.2. The hopane isomerization results are inconclusive.

The measured and modelled maturation of source rocks reveals substantial heterogeneity throughout the Termit Basin. However, the Oligocene samples studied are in general thermally immature, and only about one-half of them exhibit a thermal maturity level corresponding to the onset of the oil window ($\%R_o$ = 0.5). Most of the Paleocene samples are also thermally immature. Maastrichtian-Campanian samples are in general thermally mature but some have reached the main phase of oil generation ($\%R_o$ = 0.7). The thermal maturity of Santonian source rocks corresponds to an interval between the onset of the oil window and the main oil generation phase ($\%R_o$ = 0.7 to 1).

Exploration strategies within the Termit Basin should take into consideration the timing of maturation with respect to differing fault pathways which accompanied the tectonic pulses. This may have led to the development of hydrocarbon accumulations with differing oil-gas compositions in different reservoir compartments.

ACKNOWLEDGEMENTS

We are indebted to J. P. Passeron, formerly Manager Lake Chad/Niger, Africa/Middle East Business Unit at Exxon Exploration Company, and Dirk Laenerts (General Manager, Esso Exploration & Production Niger Inc.) who took part in the initiation of this study and gave permission to sample borehole cuttings. Special thanks are due to the Secretary General of the Ministry of Mines and Energy of Niger and his colleagues of the "Direction des Hydrocarbures", who granted authorization to conduct this research project. The American Department of State provided financial support through the Council for International Exchange of Scholars (CIES). We gratefully acknowledge Mrs Konto (American Cultural Center, Niamey), Debra Egan and Michelle Grant (Fulbright Scholar Program, Africa/Western Hemisphere). Finally, the manuscript was significantly improved following the constructive comments of Ralf Littke and an anonymous reviewer who helped the authors question the premises of their conclusions more thoroughly.

REFERENCES

ACHRAF, B., MABROUK EL ASMI, A., SKANJI A. and EL ASMI K., 2015. A new borehole temperature correction in the Jeffara basin: impact on Tannezuft source rock thermal maturity and associated hydrocarbon generation. Thirteenth Tunisian Petroleum Exploration & Production Conference, October 26-31, 4 pp.

BELLION, Y., 1989. Histoire géodynamique post-paléozoïque de l'Afrique de l'Ouest d'après l'étude de quelques bassins sédimentaires (Sénégal, Taoudenni, Iullemmeden, Tchad). *Centre International pour la Formation et les Echanges Géologiques, CIFEG,* **17**, 1-302.

CHRISTIE-BLICK, N. and BIDDLE, K. T., 1985. In: Strike-Slip Deformation, Basin Formation, and Sedimentation along

strike-slip faults. *SEPM Special Publication*, **37,** 1–34.

DOWDLE, W.L. and COBB, W. M., 1975. Static formation temperature from well logs - an empirical method. *J. Petrol. Tech*., **27,** 1326-1330.

ESPITALIÉ, J., SENGA MAKADI, K. and TRICHET, J., 1984. Role of the mineral matrix during kerogen pyrolysis. *Org. Geochem*., **6**, 365-382.

FAIRHEAD, J. D., 1986. Geophysical controls on sedimentation within the African Rift system. In: Frostick, L. E., Renault, R. W., Reid, I. and Tiercelkin, J. J., (Eds), Sedimentation in the African rifts. *Geol. Soc. Lond., Spec. Publ.*, **25**, 19-27.

FAURE, H., 1966. Reconnaissance géologique des formations sédimentaires post paléaezoïques du Niger oriental: *Memoires du Bureau de Recherches Géologiques et Minieres,* **47**, 629pp.

GAYA, M. L., 2013. Oil exploration and development in Niger. 7th Annual German-African Forum, *http://www.energyafrica.de/fileadmin/user_upload/Energy_Africa_13/Presentation_Ministry%20of%20Energy%20Niger_Gaya_Panel%205b_7th%20German-African%20Energy%20Forum%202013.pdf,* accessed 19 Nov 2016.

GENIK, G. J., 1992. Regional framework, structural and petroleum aspects of rift basins in Niger, Chad, and the Central African Republic. *Tectonophysics*, **213** (1-2), 169-185.

GENIK, G. J., 1993. Petroleum Geology of Cretaceous-Tertiary rift basins in Niger, Chad and Central African Republic. *AAPG Bull*., **77**, (8), 1405-1434.

GREIGERT, J., 1978. Atlas des eaux souterraines du Niger : état des connaissances. Rapport BRGM 79AGE001, Tomes 1 et 2. Orléans, France.

HAROUNA, M. and PHILP, R. P., 2012. Potential petroleum source rocks in the Termit basin, Niger. *Journ. Petrol. Geol.,* **35** (2), 165-186.

HUNT, J. M., 1996. Petroleum Geochemistry and Geology, New York: W. H. Freeman and Company, 743p.

KRUGE, M.A., 1983. Diagenesis of Miocene biogenic sediments in Lost Hills oil field, San Joaquin Basin, California. In: C. M. Isaacs & R. E. Garrison, Petroleum generation and occurrence in the Miocene Monterey Formation, California (pp. 39-51). Los Angeles: The Pacific Section, Society of Economic Paleontologists and Mineralogists.

LEE, HSIEN-TSUNG and LI-CHUNG SUN, 2014. Correlation among vitrinite reflectance R_o%, pyrolysis parameters, and atomic H/C ratio: Implications for evaluating petroleum potential of coal and carbonaceous materials. *Journal of Energy and Natural Resources,* **3**(6)*, 85-100.*

LIU BANG, LUNKUN WAN, FENGJUN MAO, JIGUO LIU, MINGSHENG LU and YUHUA WANG, 2015. Hydrocarbon potential of Upper Cretaceous marine source rocks in the Termit Basin, Niger. *Journal of Petroleum Geology,* **38** (4), 157-175.

LIU BANG, GUANGYA ZHANG, FENGJUN MAO, JIGUO LIU and MINGSHENG LIU, 2017. Geochemistry and origin of Upper Cretaceous oils from the Termit Basin, Niger. *Journal of Petroleum Geology,* **40**(2), 195-207.

LOUIS, P., 1970. Contribution géophysique à la connaissance géologique du bassin du lac Tchad. Paris, ORSTOM, 1970, 2 (42), 312 p.

METWALLI, F. I. and PIGOTT, J. D., 2005. Petroleum system criticals of the Matruh-Shushan Basin, Western Desert, Egypt. *Petrol. Geosc*., **11** (2), 157-178.

MBendi Information Services, 2010. Crude petroleum and natural gas extraction in Chad-Overview: Available at *http://www.mbendi.com/indy/oilg/ogus/af/ch/p005.htm*. Accessed 19 November 2016. 2p.

McHARGUE, T. R., HEIDRICK, T. L. and LIVINGSTONE, J., 1992. Tectonostratigraphic development of the Interior Sudan Rifts, Central Africa. *Tectonophysics*, **213,** 187-202.

PETERS, K. E., 1986. Guidelines of evaluating petroleum source rocks using programmed pyrolysis. *AAPG Bull.,* **70**(3), 318-329.

PIGOTT, J.D. and ABOUELRESH, M.O., 2016. Basin deconstruction-construction: Seeking thermal-tectonic consistency through the integration of geochemical thermal indicators and seismic fault mechanical stratigraphy-Example from Faras Field, North Western Desert, Egypt. *Journal of African Earth Sciences*, **114**, 110-124.

PIGOTT, J.D. and SATTAYARAK, N., 1993. Aspects of sedimentary basin evolution assessed through tectonic subsidence analysis, example: Northern Gulf of Thailand. *Journ. Southeast Asian Earth Sci*., **8**, 1-4, 407-420.

PIGOTT, J.D., OMER AKSU, and AHMED ALAHDAL, 2008. Basin Analysis of Southern Yemen Red Sea: Significance of Halokinesis Upon Subsalt Source Rock Maturities and Hydrocarbon Migration Dynamics. In: GEO 2008, 8th Middle East Geoscience Conference and Exhibition, Bahrain.

RECHENMANN, J., 1967. Réseau de bases magnétiques au Niger et au Tchad occidental 1962-1965, en Afrique occidentale 1959-1962. Cahiers ORSTOM, Sér. Geophys., 8, Paris

RECHENMANN, J., 1969. Cartes gravimétriques du Niger. Notice explicative 36, ORSTOM, Paris.

RU, K. and PIGOTT, J. D., 1986. Episodic rifting and subsidence in the South China Sea. *AAPG Bull.,* **70** (9), 1136–1986.

RULLKOTTER, J. and MARZI, R., 1988, Natural and artificial maturation of biological markers in a Toarcian shale from northern Germany. In: L. Mattaveilli and L. Novelli (Eds), *Advances in Geochemistry 1987.* Pergamon Press, Oxford, pp. 639-645.

SCHULL, T. J., 1988. Rift basins of interior Sudan, petroleum exploration and discovery. *AAPG Bull*., 72, 1128 - 1142.

SWEENEY, J., TALUKDAR, S., BURNHAM, A. and VALLEJOS C., 1990. Pyrolysis kinetics appled to prediction of oil generation in the Maracaibo Basin, Venezuela, Proceedings of the 14th *International Meeting on Organic Geochemistry,* **16**, 189-196.

TEICHMÜLLER, M. and DURAND, B., 1983. Fluorescence in microscopical rank studies on liptinites and vitrinites in peat and coals, and comparison with the results of the Rock-Eval pyrolysis. *Int. J. Coal Geol*., **2**, 197-230.

TISSOT, B. P. and WELTE, D. H., 1984. Petroleum formation and occurrence, (2nd ed.), Berlin: Springer, pp. 223, 509-523.

TISSOT, B. P., PELET, R. and UNGERER, P. H., 1987. Thermal history of sedimentary basins, maturation indices, and kinetics of oil and gas generation. *AAPG Bull*., **71**, 1445 -1466.

VANDENBROUCKE, M., DURAND, B. and OUDIN, J. L., 1983. Detecting migration phenomena in a geological series by means of C_1-C_{35} hydrocarbon amounts and distributions. In: M. Bjoroy *et al.* (Eds.). *Advances in Organic Geochemistry 1982*, pp. 147-155. Chichester, Wiley.

WAN, L. K., LIU, J. G., MAO, F. J., LU, M. S. and LIU, B., 2014. The petroleum geochemistry of the Termit Basin, Eastern Niger, *Marine and Petroleum Geology*, 51, 167–183.

WAPLES, D., 1985. Geochemistry in petroleum exploration. Reidel Publishing Company.

ZANGUINA, M., BRUNETON, A. and GONNARD, R., 1998. An introduction to the petroleum potential of Niger. *Journ. Petrol. Geol.,* **21** (1), 83-103.